The Journal of Experimental Medicine

Activation of Microglial Poly(ADP-Ribose)-Polymerase-1 by Cholesterol Breakdown Products during Neuroinflammation: a Link between Demyelination and Neuronal Damage

Antje Diestel,[1] Orhan Aktas,[2] Dagmar Hackel,[1] Ines Häke,[1] Susanne Meier,[2] Cedric S. Raine,[3] Robert Nitsch,[1] Frauke Zipp,[2] and Oliver Ullrich[1,4]

[1]*Department of Cell and Neurobiology, Institute of Anatomy, and* [2]*Institute of Neuroimmunology, Clinical and Experimental Neuroimmunology, University Hospital Charité, 10098 Berlin, Germany*
[3]*Albert Einstein College of Medicine, New York, NY 10461*
[4]*Institute of Immunology, University Hospital Magdeburg, 39120 Magdeburg, Germany*

Abstract

Multiple sclerosis (MS) is a chronic demyelinating disease in which it has only recently been suggested that damage to neuronal structures plays a key role. Here, we uncovered a link between the release of lipid breakdown products, found in the brain and cerebrospinal fluid (CSF) of MS patients as well as in experimental autoimmune encephalomyelitis, and neuronal damage mediated by microglial activation. The concentrations of the breakdown product 7-ketocholesterol detected in the CSF of MS patients were capable of inducing neuronal damage via the activation and migration of microglial cells in living brain tissue. 7-ketocholesterol rapidly entered the nucleus and activated poly(ADP-ribose)-polymerase (PARP)-1, followed by the expression of migration-regulating integrins CD11a and intercellular adhesion molecule 1. These findings reveal a novel mechanism linking demyelination and progressive neuronal damage, which might represent an underlying insidious process driving disease beyond a primary white matter phenomenon and rendering the microglial PARP-1 a possible antiinflammatory therapeutic target.

Key words: multiple sclerosis • glia • neurodegeneration • encephalomyelitis • integrins

Introduction

Multiple sclerosis (MS) is a chronic demyelinating disease in which it has only recently been suggested that damage to neuronal structures plays a key role (1–10). In addition to demyelination and damage to oligodendrocytes, the primary and quantitatively dominating histopathological characteristics of MS, axonal damage (6, 8–10), and neuronal cell death (5) have recently been reemphasized in MS patient brain tissue. Because there is evidence that the severity of MS sometimes correlates better with neuronal alterations than with demyelination (10), the mechanisms linked to this neuronal pathology could serve as promising targets for therapeutic improvements in the clinical outcome of the disease.

During the development of MS, myelin sheaths are preferentially and extensively damaged by an attack of immune cells in multiple areas of the brain and spinal cord (11). This attack involves the release of large amounts of free oxygen radicals, which contribute to the radical-mediated oxidation and breakdown of myelin (12, 13). Because cholesterol is a major component of the myelin sheath, and cholesterol oxidation products are well known for exhibiting cytotoxic effects toward blood vessels (14–16) and neurons (17–19), we addressed the question of whether such products could induce and maintain neuronal cell damage after the initial immune attack in MS.

A. Diestel, O. Aktas, and D. Hackel contributed equally to this work.
R. Nitsch, F. Zipp, and O. Ullrich contributed equally to this work.

Address correspondence to Oliver Ullrich, Department of Cell and Neurobiology, Institute of Anatomy, Medical Faculty Charité, Humboldt-University Berlin, Philippstr. 12, 10115 Berlin, Germany. Phone: 49-30-450-528245; Fax: 49-30-450-528300; email: oliver.ullrich@charite.de

Abbreviations used in this paper: BHT, β-hydroxytoluol; CNS, central nervous system; CSF, cerebrospinal fluid; DTT, dithiothreitol; EAE, experimental autoimmune encephalomyelitis; GC/MS, gas chromatography/mass spectrometry; HPLC, high performance liquid chromatography; ICAM, intercellular adhesion molecule; iNOS, inducible nitric oxide synthase; MS, multiple sclerosis; NF, nuclear factor; OHSC, organotypic hippocampal slice culture; OND, other neurological disease; PARP, poly(ADP-ribose)-polymerase; w.w., wet weight.

 J. Exp. Med. © The Rockefeller University Press • 0022-1007/2003/12/1729/12 $8.00
Volume 198, Number 11, December 1, 2003 1729–1740
http://www.jem.org/cgi/doi/10.1084/jem.20030975

Materials and Methods

Sample Collection. Serum, cerebrospinal fluid (CSF), and PBMCs of donors were collected at the Institute of Neuroimmunology and the Department of Neurology, University Hospital Charité, Berlin, Germany. The study was approved by the local ethical committee. Of the 23 patients, 11 had been diagnosed with relapsing remitting MS, according to Poser's criteria (20). The other 12 patients had other inflammatory and noninflammatory neurological diseases (ONDs; e.g., idiopathic epilepsy, hydrocephalus, migraine, trigeminal neuralgia, multiple systemic atrophy, cerebral infarction, torticollis, chronic headache, and polyneuropathy). All were newly diagnosed patients who had not been treated before venous puncture. Fresh frozen blocks of autopsied brain tissue from patients with chronic active MS ($n = 3$), chronic silent MS ($n = 6$), and control patients ($n = 7$) were provided by C.S. Raine on dry ice (mean postmortem delay: 8.0 + 0.0 h for patients with chronic active MS, 3.5 + 0.9 h for patients with chronic silent MS, and 7.6 + 1.3 h for control patients). Central nervous system (CNS) tissue from chronic active cases contained established, gliotic lesions with evidence of recent inflammatory activity at the lesions margins, and some fresh, acute MS lesions with edema, actively demyelinating margins rich in inflammatory cells, and numerous hypertrophic astrocytes. Chronic silent cases displayed lesions that were intensely gliotic and demyelinated with little evidence of inflammation (21). The 16 brain samples were assigned numbers and studied for 7-ketocholesterol by investigators blinded to the code.

Detection of Oxysterols in the CSF. Cholesterol oxidation products in the serum and CSF of the patients were analyzed by gas chromatography/mass spectrometry (GC/MS) as described by Sevanian et al. (22). In brief, 5 mg/liter 5α-cholestane was added as the internal standard to 200 μl serum or CSF, and lipids were extracted and then fractionated by a diol column. The cholesterol/cholesterol oxide fraction was then subjected to alkaline hydrolysis in ether, extracted, methylated using etheral diazomethane, and derivatized to trimethylsilylethers with bis(trimethylsilyl)-trifluoroacetamide in dimethylformamide. All extraction and derivatization procedures were performed in 0.01% β-hydroxytoluol (BHT) and in an argon atmosphere to prevent further oxidation during the sample preparation for GC/MS. Because the human CSF samples have to be subjected to diagnostic investigations, BHT was added after taking the aliquot for 7-ketocholesterol analysis. Control experiments demonstrated no differences between an immediate addition of BHT and adding BHT before starting the extraction procedure. Samples were analyzed on a Shimadzu gas chromatograph coupled with a mass spectrometer (180°C for 5 min, 4°C/min, and 260°C for 5 min), and mass chromatograms were recorded in the mass range from 130–700 mass to charge ratio at a scan rate of three scans per second. Peak identification was based on relative retention time and ion mass spectrometry in comparison with external standards and quantified by integration in relation to the internal standard.

Detection of 7-Ketocholesterol by High Performance Liquid Chromatography (HPLC). Cholesterol oxidation products were analyzed by a reverse phase HPLC method as described by Kritharides et al. (23) after extraction as described above. The concentrations of total cholesterol in serum were 1.58 ± 0.32 g/liter for control patients and 1.72 ± 0.40 g/liter for MS patients. The cholesterol concentration in the CSF was 6.83 ± 1.88 mg/liter for control patients and 8.35 ± 2.73 mg/liter for MS patients.

Induction and Clinical Evaluation of Active Experimental Autoimmune Encephalomyelitis (EAE). 6–8-wk-old female SJL mice (~20 g body weight; Charles River Laboratories) were immunized s.c. with 75 μg proteolipid protein 139–151 (purity >95%; Pepceuticals) in 0.2 ml emulsion consisting of equal volumes of PBS and CFA (Difco) and containing 6 mg/ml *Mycobacterium tuberculosis* H37Ra (Difco). 200 ng pertussis toxin (List Biological Laboratories) was administered i.p. at days 0 and 2. Mice were daily scored for EAE (24) as follows: 0, no disease; 1, tail weakness; 2, paraparesis; 3, paraplegia; 4, paraplegia with forelimb weakness or paralysis; 5, moribund or dead animals (25). Clinical scores on separate days and mean maximal scores were calculated by adding scores of individual mice and dividing by number of mice in each group. All procedures were conducted according to protocols approved by the local animal welfare committee.

Immunohistochemistry and Quantitative Assessment. Mice killed with narcotics were transcardially perfused with 4% paraformaldehyde. Horizontal 50-μm thick vibratome sections (Shandon) were immersed with 3% H_2O_2 to quench unspecific endogenous peroxidase activity, washed, and blocked (10% normal serum and 0.5% Triton X-100) before overnight incubation with anti-active caspase 3 (1:100; R&D Systems). Sections were immunolabeled using the avidin/biotinylated enzyme complex technique (ABC-Elite; Vector Laboratories) before development with diaminobenzidine (brown signal) as substrate. Ig control experiments were performed for all primary antibodies and no staining was observed under these conditions. Section were counterlabeled by Nissl staining. Neurons positive for active caspase 3 were counted in brain stem sections by two independent investigators in a blind manner. Four visual fields on both sides of the midline in the brain stem motor area were counted for caspase-3^+ neurons using a ×20 objective. The average number of neurons from three animals, with four sections analyzed per mouse, is shown as relative to the controls in Fig. 3 a.

Cell Culture. BV-2 microglial cells are primary mouse microglial cells immortalized by stabile transfection with the *c-myc*-oncogene using a J7-retrovirus (26), leading to a phenotype functionally identical to native primary microglia (27). These cells were cultured in DMEM medium supplemented with 16% FCS at a density not exceeding 2×10^5 cells/ml. Microglial activation was performed by incubation with 10 μg/ml LPS (Sigma-Aldrich) for 24 h. Primary neurons were prepared from 10-d-old mice, the brain tissue were dissociated with 0.25% trypsin, centrifuged at 470 *g* for 10 min, resuspended in neurobasal medium, plated on poly-L-lysin–coated 24-well plates, and incubated at 37°C, 5% CO_2 and 95% air. After appearance of a confluent cell layer, adherent glia cells will be mechanically dissolved and the proliferation of the remaining glia cells will be inhibited by 8 μM cytosine arabinoside for 3 d. HT22 hippocampal neurons were cultured in DMEM medium supplemented with 10% FCS and 8.5 g/liter glucose at a density of 10^5 cells/ml or lower. To investigate $CD3^+$ T cells and $CD14^+$ monocytes, PBMCs of four healthy donors were isolated from fresh blood by Lymphoprep™ density gradient centrifugation (Nycomed Pharma AS) and separated using immunomagnetic beads according to the manufacturer's instructions (Miltenyi Biotec). For analyzing 7-ketocholesterol, cells were left untreated or stimulated with 1 μg/ml coated anti-CD3 (provided by Janssen-Cilag) and 25 μg/ml anti-CD28 (R&D Systems) or 50 ng/ml LPS (Sigma-Aldrich).

Incubation of BV-2 Microglial Cells with 5-Cholesten-3β-Ol-7-One (7-Ketocholesterol). Murine BV-2 microglial cells, which exhibit the functional features of primary microglia, were incubated for 24 h with 0, 1, 10, and 100 mg/liter 5-cholesten-3β-ol-7-one (7-ketocholesterol) at a density of 10^6 cells/culture flask in 20 ml DMEM medium, supplemented with 10% FCS. All experiments

were performed using a vehicle control. 7-ketocholesterol was initially dissolved in ethanol, but cell culture medium containing 7-ketocholesterol was produced by completely removing the solvent under a nitrogen stream and redissolving the remaining material in cell culture medium supplemented with FCS. Immediately before incubating the cell or brain tissue, the 7-ketocholesterol concentration was confirmed by HPLC analysis. The vehicle control was subjected to the same procedure.

Biochemical Analyses. FACS® analysis was performed with FITC-conjugated monoclonal rat anti–mouse-CD11a, rat anti–mouse-CD11b, rat anti–mouse-CD18, and rat anti–mouse intercellular adhesion molecule (ICAM)-1 antibodies (BD Biosciences). Cells were lysed by repeated freeze thawing cycles, and then the lysates were used for experiments. Nuclei were isolated by a modification of the method by Emig et al. (28) and lysed by repeated freeze thawing cycles in 1 mM dithiothreitol (DTT). Poly(ADP-ribosyl)ation activity was measured as the incorporation of radioactivity from ^{32}P-NAD$^+$ into trichloroacetic acid-insoluble material. The reaction mixture contained 100 mM phosphate buffer, pH 7.8, 200 μM NAD$^+$, 10 mM $MgCl_2$, 5 mM DTT, 1 mM DTT, 1 μg sonicated DNA/reaction, and 500,000 dpm ^{32}P-NAD$^+$ (NEN Life Science Products). In vitro poly(ADP-ribosyl)ation was detected by incubation of 2 μg recombinant poly(ADP-ribose)-polymerase (PARP)-1 expressed in *Escherichia coli* (Qbiogene) with and without native or sonified pcDNA3.1-vector-DNA. SDS/PAGE analysis was performed in a 12% separation gel, after which the separated proteins were transblotted onto nitrocellulose membranes. The membranes were incubated with antibodies directed against nuclear factor (NF)-κB (p65; Upstate Biotechnology), inducible nitric oxide synthase (iNOS; Sigma-Aldrich), and PARP (BIOMOL Research Laboratories, Inc.). After incubation with an appropriate peroxidase-conjugated secondary antibody, the blots were developed with a chemiluminescence detection kit (Amersham Biosciences).

Experiments with Organotypic Hippocampal Slice Cultures (OHSCs). OHSCs were obtained by decapitating newborn mice on the 9–10th postnatal day, aseptically removing a frontal slice of the caudal cerebrum, and transversally sectioning it at a thickness of 350 μm on a sliding vibratome in MEM supplemented with 1% L-glutamine as previously described (29). OHSCs were cultivated in culture medium (MEM/HBSS 2:1, 25% normal horse serum, 2% L-glutamine, 2.64 mg/ml glucose, and penicillin/streptomycin) at 35°C with 5% CO_2 for 10 d in vitro to ensure a healthy organotypic microenvironment in the middle layer, which is known to induce microglial ramification (29). For the detection of 7-ketocholesterol after excitotoxic injury, OHSCs were exposed to 50 μM NMDA, after which the medium was removed and the tissue was harvested for further analysis. 3 d after transfer of microglial cells (BV-2 microglial cells, pcDNA3.1.-BV-2 microglial cells, or antisense-PARP-1-pcDNA3.1-BV-2 microglial cells, respectively; reference 27) in the presence or absence of 10 mg/liter 7-ketocholesterol, cell death in the sites of neuronal injury (neuronal cell layers of CA and DG) was detected by staining with 5 μg/ml propidium iodide for 4 h (27) and was quantified in the cryostat sections (29). Neurons were identified by double fluorescence staining against the neuronal nuclear protein NeuN (1:1,000; mouse anti–mouse; Chemicon) or neurofilament (1:1,000; mouse anti–mouse; Chemicon). Microglia were labeled immunohistochemically by Griffonia simplicifolia isolectin IB_4 (IB_4)-FITC (diluted 1:40; Sigma-Aldrich) in 0.1 M phosphate buffer, pH 6.8, and 0.5% Triton X-100. The material was examined with a BX-50 microscope (Olympus). Fluorescence was evaluated with the following filters: for FITC, excitation filter 470–490 nm, barrier filter 515–550 nm; for rhodamine, excitation filter 520–550 nm, barrier filter 580 nm. Site-specific migration of BV-2 microglial cells into the regions of neuronal layers of OHSCs were quantified as the ratio between the cell count of Mini-Ruby–prelabeled vector-control-BV-2 microglia cells or antisense-PARP-1-BV-2 microglial cells in the neuronal layers (27).

Results

Accumulation of 7-Ketocholesterol in the CSF of MS Patients. We analyzed serum and CSF of patients with MS and patients with ONDs using a GC/MS method for identification and quantification of cholesterol oxides (22). All patients were newly diagnosed and had not received any previous treatment. Cholesterol oxides were detected in high concentrations in the CSF of MS patients, whereas OND patients revealed only very low or no detectable amounts. The major cholesterol oxidation product in the CSF was identified as 5-cholesten-3β-ol-7-one (7-ketocholesterol) by ion mass spectrometry in comparison with known standards. We found a distinctly elevated concentration of 7-ketocholesterol in the CSF of MS patients compared with OND patients (Fig. 1 a). The CSF/serum ratio (Fig. 1 b) indicates that the detected 7-ketocholesterol originated from the CNS and not the blood system (16, 22, 30). In fact, we did not find direct release of 7-ketocholesterol from activated mononuclear cells (CD3$^+$ T cells activated with CD3/CD28, CD14$^+$ monocytes activated with LPS) up to 72 h after stimulation, indicating brain tissue as the source of 7-ketocholesterol (unpublished data). Although serum analysis by isotope dilution mass spectrometry (31) revealed lower 7-ketocholesterol concentrations, the detected serum concentrations in our study were fully comparable to the concentrations previously reported for healthy human subjects in studies using the GC/MS method by Sevanian et al. (22), as well as gas chromatography with flame ionization detection (32, 33).

Accumulation and Degradation of 7-Ketocholesterol in Brain Tissue. Cholesterol is not only a component of myelin, but is also localized within the outer cell membrane of neurons and nonneuronal cells, where its breakdown products can easily diffuse into the intercellular space (34) and the CSF. Therefore, in MS it might be possible that either the downstream release of large amounts of oxygen free radicals after neuronal injury or the oxidative burst by inflammatory cells contribute to the oxidative damage (35–37) and breakdown of cholesterol in the cell membrane. Thus, using HPLC (23), we analyzed the CSF of patients with neurodegenerative diseases without any clinically detectable neuroinflammation (e.g., Alzheimer's, systemic atrophy), of patients with primary and severe neuroinflammatory diseases (e.g., severe meningitis and viral encephalitis), of control patients without any CNS disease (e.g., prolapsed intervertebral disc, peripheral polyneuropathy), and of MS patients (Fig. 1 c). Although no accumulation of 7-ketocholesterol could be detected in patients with neurodegeneration (mean = 0.47 mg/liter plus 0.47 mg/liter SEM, $n = 6$), it was found

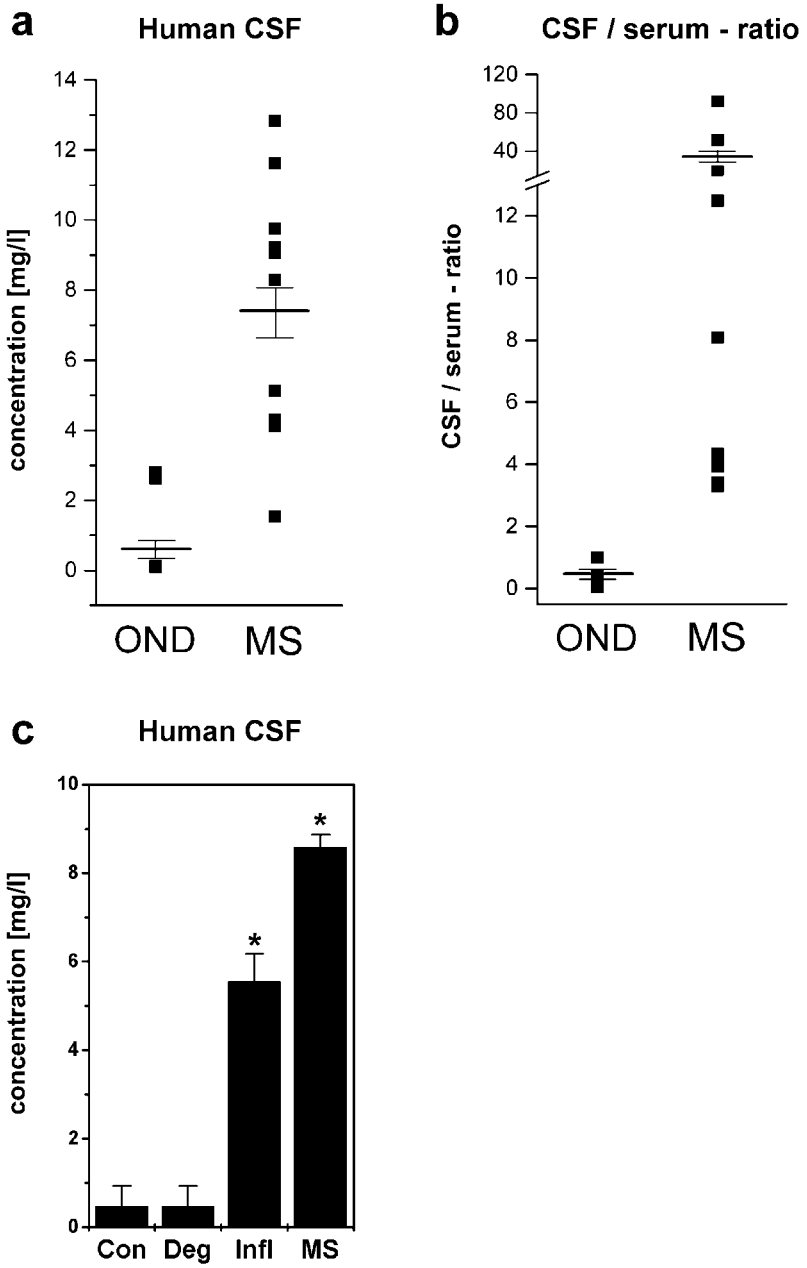

Figure 1. Assessment of 5-cholesten-3β-ol-7-one (7-ketocholesterol) in the CSF of patients with MS and in neural cell and tissue cultures. (a) Detection of 5-cholesten-3β-ol-7-one (7-ketocholesterol) in the CSF of patients with MS. Absolute 7-ketocholesterol concentrations detected by GC/MS are demonstrated for each individual MS or OND patient. Means are given as ± SEM. MS patients: mean = 7.37 mg/liter, SEM 0.32 mg/liter, $n = 11$; OND patients: mean = 0.53 mg/liter, SEM 0.08 mg/liter, $n = 12$. (b) Detection of 5-cholesten-3β-ol-7-one (7-ketocholesterol) in the CSF of patients with MS. CSF/serum ratio of 7-ketocholesterol detected in the CSF and in serum from MS and OND patients are demonstrated for each individual patient. MS patients: mean = 33.4 ± 5.12 SD, $n = 11$; OND patients: mean = 0.53 ± 0.08 SD, $n = 12$. (c) 5-cholesten-3β-ol-7-one (7-ketocholesterol) in the CSF of patients with nondemyelinating neurological diseases (neuroinflammatory diseases, neurodegenerative diseases, and control patients without CNS disease). Absolute 7-ketocholesterol concentrations in the CSF detected by HPLC are demonstrated for each group. Means are given as ± SD. Patients with MS: mean = 8.50 mg/liter ± 0.29 mg/liter, $n = 11$; neuroinflammatory diseases: mean = 5.55 mg/liter ± 0.63 mg/liter, $n = 6$; patients with neurodegenerative diseases: mean = 0.47 mg/liter ± 0.47 mg/liter, $n = 6$; patients without CNS disease: mean = 0.47 mg/liter ± 0.47 mg/liter, $n = 6$.

in substantially high concentrations in the CSF of patients with severe neuroinflammation (mean = 5.55 mg/liter plus 0.63 mg/liter SEM, $n = 6$), and of patients with MS (mean = 8.50 mg/liter plus 0.29 mg/liter SEM, $n = 11$). This suggests that 7-ketocholesterol accumulates after damage to nonneuronal cells rather than after primary neuronal damage. Interestingly, neuronal damage has also been observed in primary inflammatory CNS diseases like meningitis (38), but it follows the initial nonneuronal pathology.

To find out whether 7-ketocholesterol is produced during active inflammation, we assessed the concentration of 7-ketocholesterol in an inflammatory environment in living brain tissue. We used OHSCs incubated with microglial cells with and without stimulation by LPS, allowing these cells to invade living brain tissue. Inflammation itself might lead directly to either an additional endogenous release of 7-ketocholesterol from brain tissue induced by invading microglial cells, a disturbance of supposed detoxifying metabolisms in brain tissue by these microglial cells, or both. In these experiments, endogenous 7-ketocholesterol strongly accumulated in living brain tissue invaded by microglial cells (Fig. 2 a), but disappeared quickly after reaching a maximum after 8 h, indicating the existence of a 7-ketocholesterol degrading system. In brain tissue incubated with 10 mg/liter 7-ketocholesterol, ~68 plus 7.8% of the initial concentration could be detected after 3 d of incubation, but disappeared completely after 3 d in brain tissue invaded by microglial

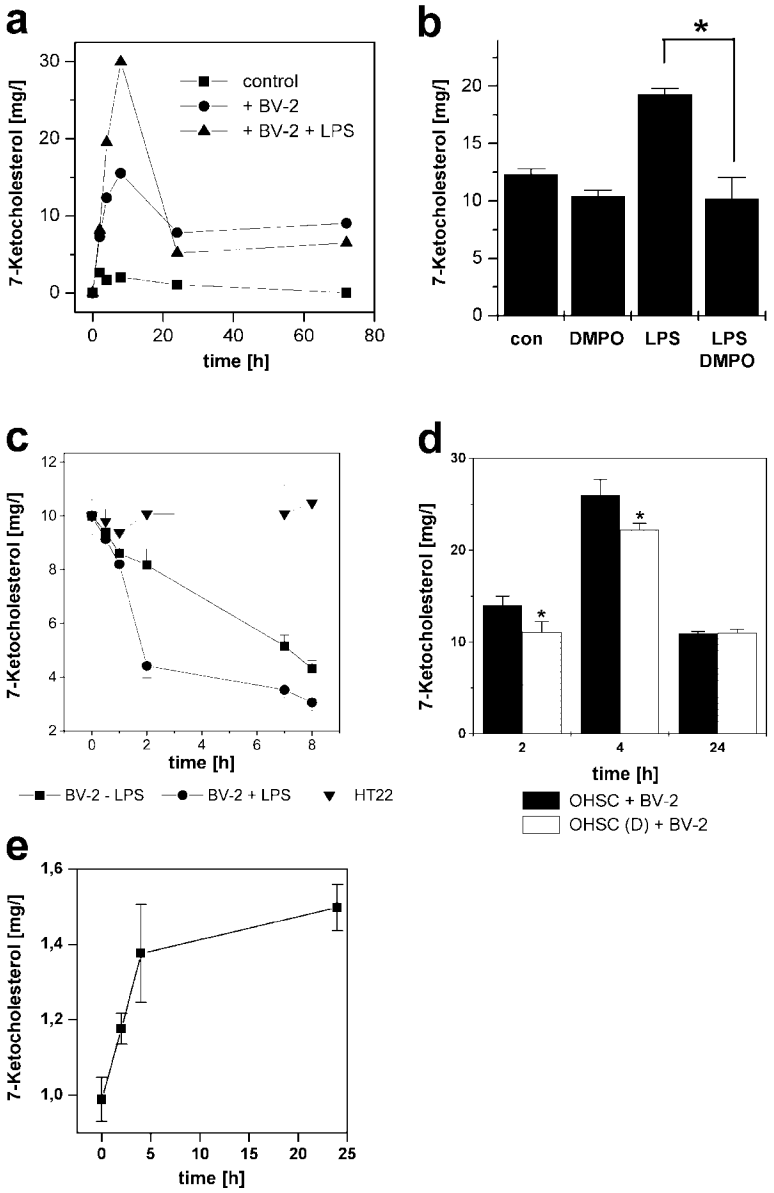

Figure 2. Accumulation and degradation of 7-ketocholesterol in brain tissue. (a) Production of 7-ketocholesterol in hippocampal brain slice cultures after invasion of microglial cells. Concentration of 7-ketocholesterol in the living brain tissue of hippocampal slice cultures after transfer of 10^5 BV-2 microglial cells with (+BV-2 +LPS) or without (+BV-2) previous activation by LPS in comparison to untreated controls (control). Data are given as mean, SD $<$ 10%, $n = 6$. (b) Influence of oxygen radicals on the concentration of 7-ketocholesterol in hippocampal brain slice cultures. Concentration of 7-ketocholesterol in the living brain tissue of hippocampal slice cultures 4 h after transfer of 10^5 BV-2 microglial cells with (LPS) or without (con) previous activation by LPS or incubation with 75 mM of the extracellular radical scavenger, DMPO. Data are given as mean $\pm$ SD, $n = 6$. *, $P < 0.005$. (c) Degradation of 7-ketocholesterol. Degradation of 7-ketocholesterol by BV-2 microglial cells with (■) or without (●) previous activation by LPS and HT22 hippocampal neurons (▼). Data are given as concentrations in the cell culture supernatant. Data are given as mean $\pm$ SD, $n = 6$. (d) Production of 7-ketocholesterol from nonneuronal components of hippocampal brain slice cultures after invasion of microglial cells. Concentration of 7-ketocholesterol in the living brain tissue of hippocampal slice cultures after transfer of 10^5 LPS-activated BV-2 microglial cells (OHSC). OHSC(D), previous elimination of living neurons by incubation with 50 μM NMDA for 24 h. Data are given as mean $\pm$ SD, $n = 6$. *, $P < 0.05$. (e) Production of 7-ketocholesterol by NMDA-damaged primary neurons. The release of 7-ketocholesterol in the culture medium after induction of neuronal damage by 50 μM NMDA is demonstrated. Data are given as mean $\pm$ SD, $n = 6$.

cells (2.1 $\pm$ 0.4%), implying rapid degradation by microglial cells. LPS activation of microglial cells resulted in a fast and substantial accumulation of 7-ketocholesterol in the brain tissue, but also in an even faster disappearance afterwards (Fig. 2 a). The rapid decline of the 7-ketocholesterol content in OHSCs invaded by microglial cells suggests that microglial cells could be capable of both uptake and degradation of 7-ketocholesterol. In fact, we could show that HT22 neuronal cells were not capable of degrading 7-ketocholesterol, although we revealed strong metabolism in BV-2 microglial cells induced by LPS (Fig. 2 c). This demonstrates a dual role of microglial cells in the inflammatory environment: induction of accumulation and degradation of 7-ketocholesterol. This fast and activation-dependent metabolism of 7-ketocholesterol could also explain why we could not detect a release by activated inflammatory cells in culture.

Moreover, coincubation with the selective extracellular free radical scavenger DMPO distinctly reduced 7-ketocholesterol release (Fig. 2 b), particularly after incubation with LPS-activated microglial cells, demonstrating its oxygen radical-derived origin. These experiments indicate that 7-ketocholesterol in brain tissue derives from the oxidative attack of microglial cells.

To investigate the contribution of neuronal and nonneuronal cells to the 7-ketocholesterol release from living organotypic brain slices after invasion of microglial cells, we compared the release of 7-ketocholesterol from these slices with the release from slices after elimination of viable neurons by incubation with 50 μM NMDA for 24 h. The complete elimination of viable cells in the neuronal layers was confirmed by propidium iodide staining. The observed difference between the 7-ketocholesterol release from the slice cultures with (~220 μg/mg protein;

Fig. 2 d) and without viable neurons (~185 μg/mg protein; Fig. 2 d) equals the amount of 7-ketocholesterol released during the NMDA-induced death of cultivated primary neurons (~40 μg/mg protein; Fig. 2 e). Thus, we provide evidence for the mainly nonneuronal source of 7-ketocholesterol that we can detect in the CSF of MS patients.

7-Ketocholesterol in Brain Tissue Correlates with Disease Score and Neuronal Damage During EAE. Presuming, as our studies indicate, that 7-ketocholesterol is formed mainly by the nonneuronal compounds of the CNS, the question arises whether 7-ketocholesterol is also detectable in MS brain tissue. We found ~2.6 times more 7-ketocholesterol in patients displaying acute MS lesions than in brain tissue of patients with chronic silent MS lesions or without CNS disease (Fig. 3 a). Because postmortem oxysterol determinations could be influenced by autolysis and autooxidation, we investigated the production of 7-ketocholesterol in murine EAE (39, 40), a well-characterized $CD4^+$ T cell–mediated animal disease model of relapsing

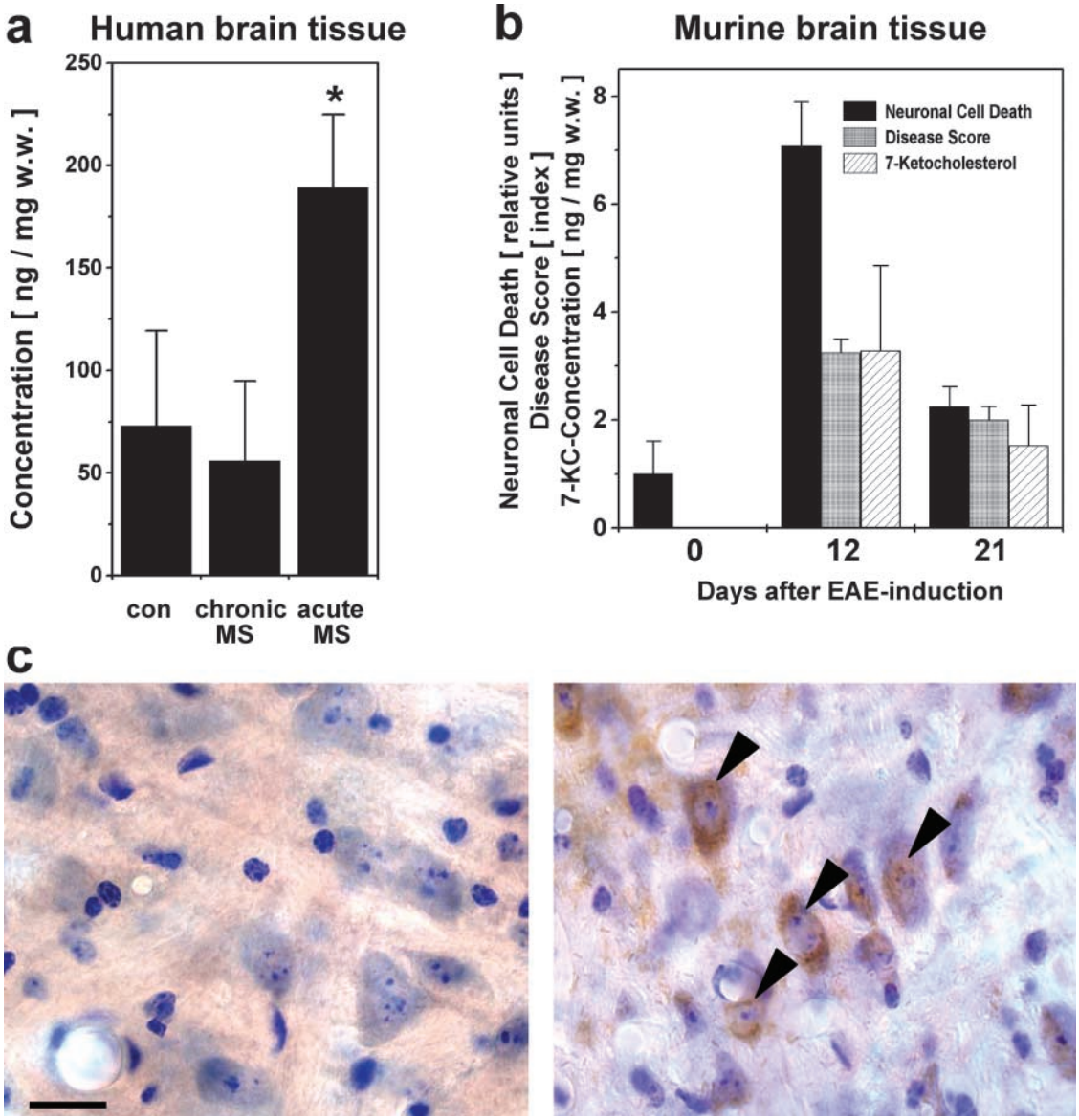

Figure 3. Accumulation of 7-ketocholesterol in CNS of MS patients and mice during EAE. (a) Detection of 5-cholesten-3β-ol-7-one (7-ketocholesterol) in brain tissue (white matter) of patients with MS. Absolute 7-ketocholesterol concentrations detected by HPLC are demonstrated for control patients and patients with chronic and acute MS. Control patients: mean = 72.8 ± 46.6 ng/mg w.w., $n = 6$; chronic MS: mean = 55.8 ± 39.0 ng/mg w.w., $n = 6$; acute MS: mean = 189.0 ± 35.7 ng/mg w.w., $n = 3$. *, $P < 0.05$. (b) Concentration of 7-ketocholesterol and neuronal cell death in the brain stem motor area and clinical disease score during the time course of EAE. Absolute 7-ketocholesterol concentrations detected by HPLC and relative amounts of active caspase-3^+ neurons are demonstrated. The clinical disease score was calculated according to Brocke et al. (reference 25). All data are given as mean from three independent experiments. (c) Active caspase-3^+ neurons in the brain stem motor area. Sections were counterlabeled by Nissl staining. Representative neurons are demonstrated for the controls (left, day 0) and the clinical peak of EAE (right, arrowheads, day 12). Bar, 20 μm.

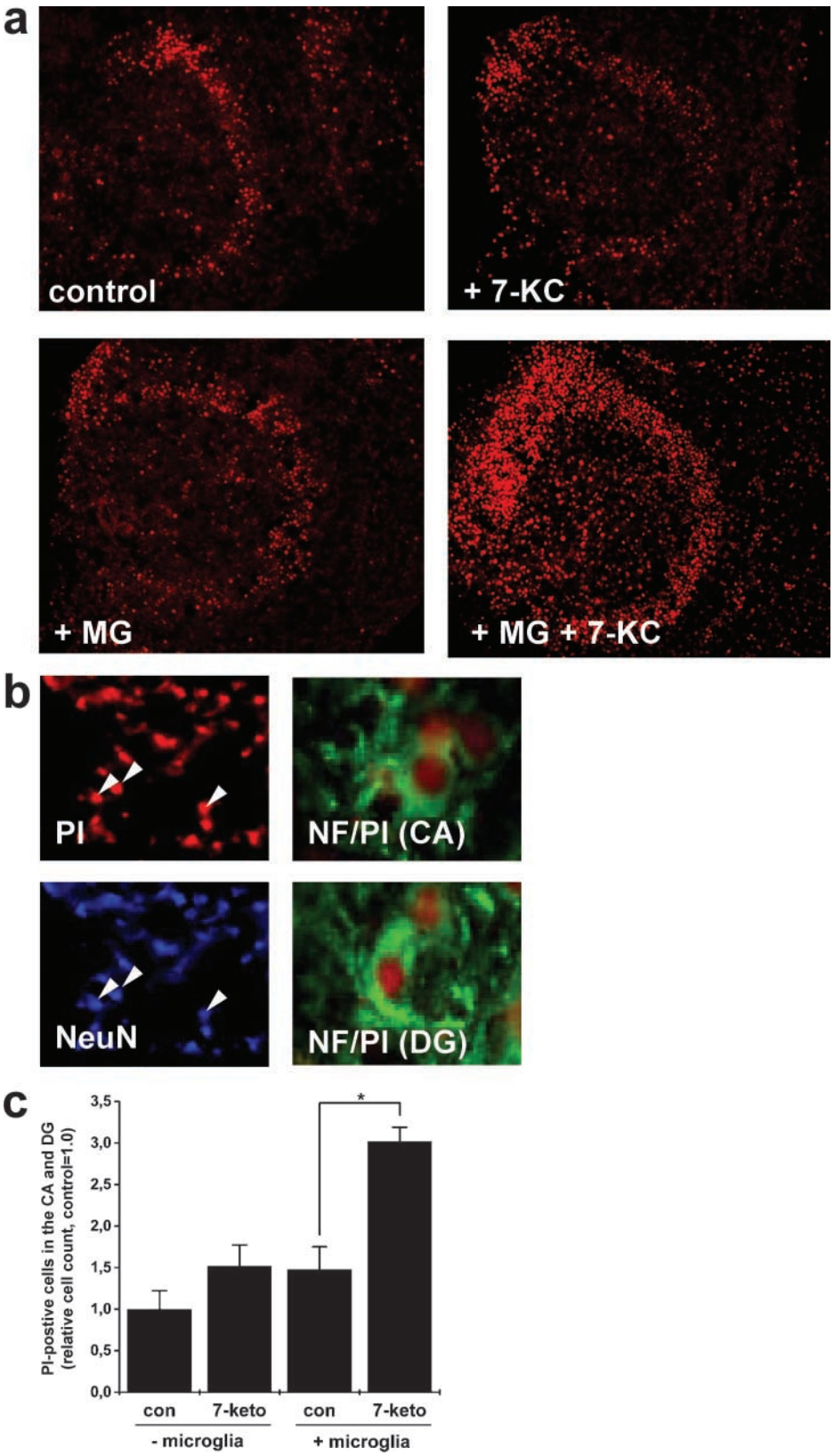

Figure 4. 7-ketocholesterol induces neuronal damage in living brain tissue mediated by microglial cells. (a) Pictures of propidium iodide fluorescence microscopy of the regions of neuronal injury in the cornu ammonis and dentate gyrus in living organotypic brain slice cultures. Control, no treatment; +MG, 3 d after transfer of 10^5 BV-2 microglial cells; +7-KC, 3 d after incubation with 10 mg/liter 7-ketocholesterol; +7-KC +MG, 3 d after incubation with 10 mg/liter 7-ketocholesterol and transfer of 10^5 BV-2 microglial cells. (b) Neuronal cell death after incubation with 7-ketocholesterol and BV-2 microglial cells. On the left: Colocalization of propidium iodide$^+$ cells (PI) with NeuN$^+$ cells (NeuN; arrowheads) in the neuronal layers of organotypic brain slice cultures after incubation with 10 mg/liter 7-ketocholesterol and transfer of 10^5 BV-2 microglial cells. On the right: Colocalization of propidium iodide$^+$ and neurofilament$^+$ cells (PI/NF) in the neuronal layers of the dentate gyrus (DG) and cornu ammonis (CA). (c) Propidium iodide$^+$ cells in the neuronal cell layer of regions of neuronal cell death (cornu ammonis and dentate gyrus). Results are given as cell counts relative to nondamaged brain tissue without transfer of cultivated microglial cells onto the slice surface (control, 1). Nonviable microglial cell counts (PI$^+$/IB$_4^+$) were subtracted. presence, 3 d after incubation with 10 mg/liter 7-ketocholesterol; + microglia, 3 d after transfer of 10^5 BV-2 microglial cells.

remitting MS (41, 42). As with its human counterpart, induction of EAE in susceptible strains of rodents leads to CNS inflammation, demyelination, and neuronal pathology (43, 44). This model system allows for correlation of clinical disease development, neuronal pathology, and accumulation of 7-ketocholesterol during the development

and clinical remission of disease. During disease development after induction of EAE, concentrations of 7-ketocholesterol increased in parallel with the level of neuronal damage in the brain stem motor area, reached their highest levels at the peak of the disease indicated by marked motor deficits and highest disease score, and subsequently decreased during clinical remission (Fig. 3, b and c). 7-ketocholesterol concentrations were elevated preferentially in tissue from those brain areas predominantly affected by EAE, such as the brain stem motor area (4.14 ± 0.71 ng/mg wet weight (w.w.) 7-ketocholesterol, compared with 1.48 ± 0.16 ng/mg w.w. 7-ketocholesterol in the nonaffected cortex). Interestingly, in animals that failed to recover completely after EAE and showed long-term neurological deficits, concentrations of 7-ketocholesterol remained elevated (Fig. 3 b), suggesting a self-sustaining mechanism of chronic inflammation.

Neuronal Damage by 7-Ketocholesterol in Living Brain Tissue Is Mediated by Microglia Cells. Next, we addressed the pathological significance of 7-ketocholesterol at the levels found in the CSF of MS patients. Several studies have reported strong neurotoxicity of cholesterol oxides in cell culture experiments (17–19). Therefore, we investigated whether 7-ketocholesterol may exhibit toxic effects toward neurons in living brain tissue (Fig. 4, a–c). In these studies, incubating OHSCs with 7-ketocholesterol for 3 d only slightly increased the rate of cell death within the neuronal layers of the hippocampus (granule cell layer of the dentate gyrus and pyramidal cell layer of the cornu ammonis). This finding argues against a direct neurotoxic effect of this cholesterol breakdown product. Because the inflammatory response in the MS brain involves activation of microglial cells, we tested the effect of 7-ketocholesterol in an inflammatory environment in living brain

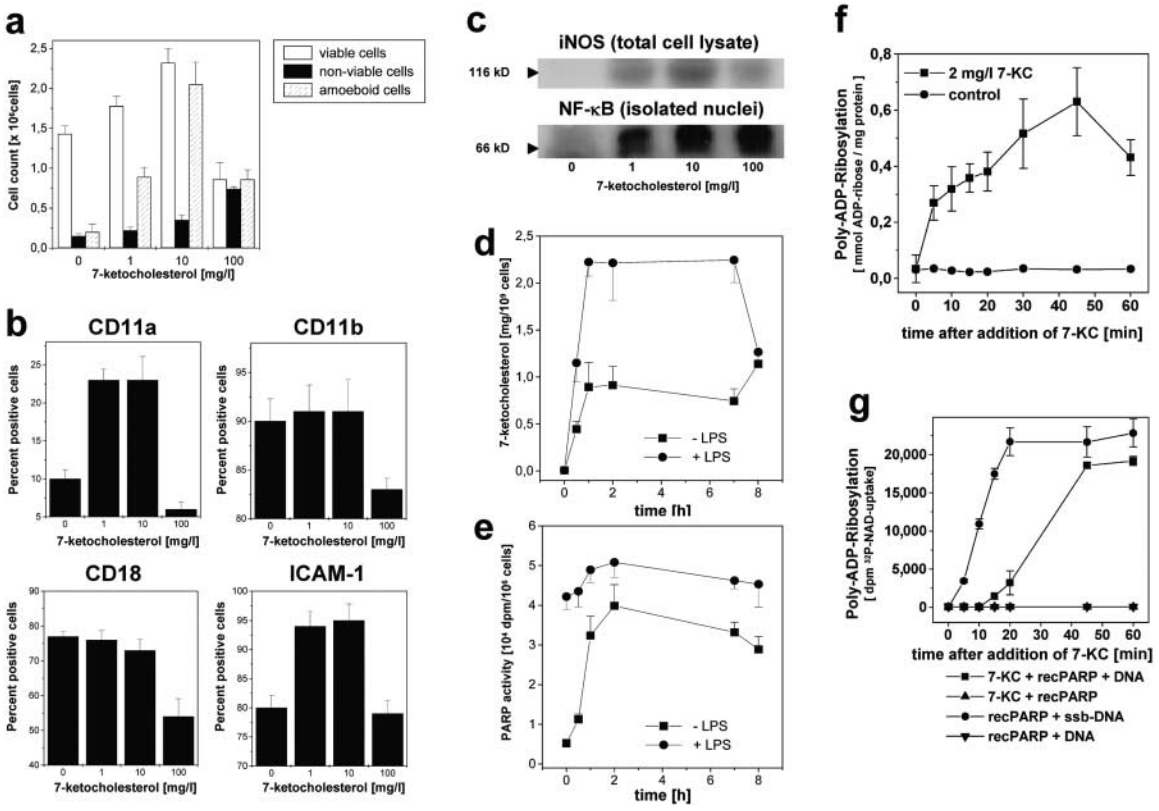

Figure 5. Induction of integrin and iNOS expression and activation of PARP by 7-ketocholesterol. (a) 7-ketocholesterol–induced alterations in morphology, proliferation, and cell death. Amoeboid, viable, and dead BV-2 microglial cells were determined after incubation for 24 h with 0, 1, 10, and 100 mg/liter 7-ketocholesterol, which represents the concentration range from stimulating to toxic concentrations. Data are given as mean ± SD, $n = 4$. (b) FACS® analysis of adhesion molecule expression. FACS® analysis of CD11a, CD11b, CD18, and ICAM-1 expression in BV-2 microglial cells after incubation for 24 h with 0, 1, 10, and 100 mg/liter 7-ketocholesterol. Data are given as positive cells ± SD, $n = 6$. (c) iNOS protein expression in cell lysates and translocated NF-κB (p65) in lysates of isolated nuclei of BV-2 microglial cells treated with 0, 1, 10, and 100 mg/liter 7-ketocholesterol. (d) Nuclear uptake of 7-ketocholesterol in BV-2 microglial cells with (+LPS) or without (−LPS) LPS treatment after incubation with exogenous 10 mg/liter 7-ketocholesterol. Data are given as mean ± SD, $n = 4$. (e) Activity of PARP in the nucleus of BV-2 microglial cells with (+LPS) or without (−LPS) LPS treatment after incubation with exogenous 10 mg/liter 7-ketocholesterol. Data are given as mean ± SD, $n = 6$. (f) Activity of PARP in isolated nuclei of BV-2 microglial cells after incubation with 2 mg/liter exogenous 7-ketocholesterol (7-KC) or with a vehicle control (control). Activity of poly(ADP-ribosyl)ation was measured as uptake of ^{32}P-labeled NAD^+ into nuclear proteins. Data are given as mean ± SD, $n = 6$. (g) Activation of isolated recombinant PARP-1 by 7-ketocholesterol is DNA dependent. Recombinant PARP-1 (recPARP) was incubated with 2 mg/liter 7-ketocholesterol (7-KC) in the presence of native (DNA) or sonified single strand break DNA (ssb-DNA). Activity of poly(ADP-ribosyl)ation was measured as uptake of ^{32}P-labeled NAD^+ into nuclear proteins. Data are given as mean ± SD, $n = 9$.

tissue. Allowing microglial cells to invade living brain tissue (27, 29) in the presence of 7-ketocholesterol, we detected severe neuronal damage with a significantly elevated rate of cell death within the neuronal layers (Fig. 4, a–c). The propidium iodide$^+$ dead cells colocalize exclusively with NeuN$^+$ cells and moreover exhibit neurofilament staining (Fig. 4 b), demonstrating that the dead cells were neurons.

Because endogenous release of 7-ketocholesterol in OHSCs induced by microglial cells (Fig. 2 a) was also not capable of inducing severe neuronal damage (Fig. 4, a and c) and 7-ketocholesterol–detoxifying metabolisms in the brain tissue were not disturbed by microglial cells (Fig. 2, a and c), we could rule out direct neuronal damage caused by 7-ketocholesterol in living brain tissue. Therefore, we came to the conclusion that the marked neuronal damage induced by

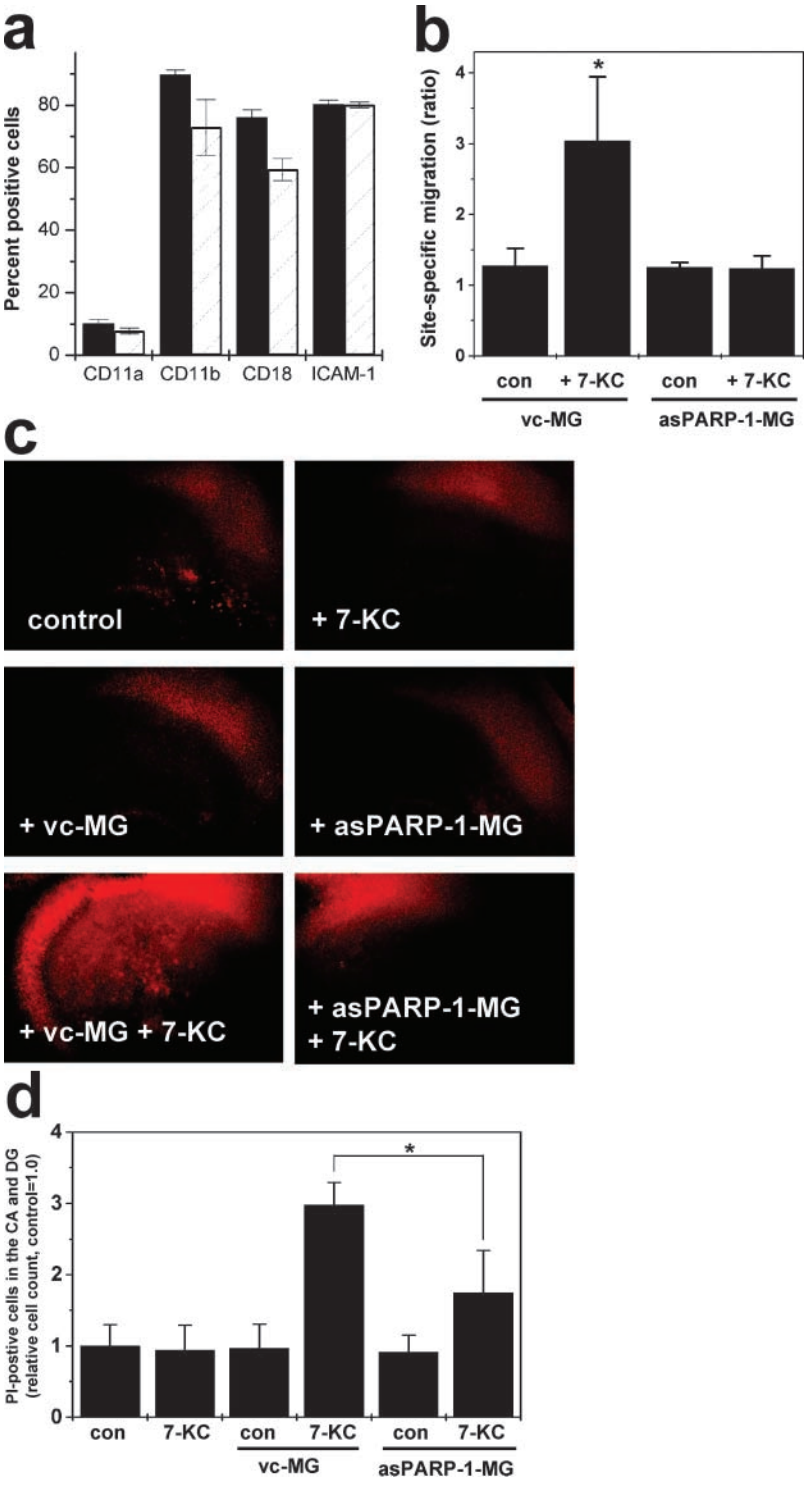

Figure 6. Induction of adhesion molecules and microglia-mediated inflammatory neuronal damage by 7-ketocholesterol depend on PARP-1. (a) FACS® analysis of CD11a, CD11b, CD18, and ICAM-1 expression in control vector-transfected BV-2 microglial cells (solid columns) and antisense PARP-1 vector-transfected BV-2 microglial cells (open columns) after incubation for 24 h with 10 mg/liter 7-ketocholesterol. Data are given as positive cells ± SD, $n = 6$. (b) Site-specific migration of BV-2 microglial cells into the regions of neuronal layers of OHSCs. Results are given as cell count of Mini-Ruby–prelabeled vector control BV-2 microglia cells (vc-MG) or antisense PARP-1 BV-2 microglial cells (asPARP-1-MG) in the neuronal layers (cornu ammonis and dentate gyrus) relative to the cell count in the nonneuronal layers. Con (control), without incubation with 7-ketocholesterol; 7-KC, 3 d after incubation with 10 mg/liter 7-ketocholesterol; + vc-MG, 3 d after transfer of 10^5 BV-2 control vector-control microglial cells; + asPARP-1-MG, 3 d after transfer of 10^5 antisense PARP-1 BV-2 microglial cells. Data are given as mean from six independent experiments ± SD. *, $P < 0.005$. (c) Propidium iodide$^+$ cells in the neuronal cell layer of regions of neurodegeneration (cornu ammonis and dentate gyrus). Results are given as cell counts relative to nondamaged brain tissue without transfer of cultivated microglial cells onto the slice surface. 7-KC, 3 d after incubation with 10 mg/liter 7-ketocholesterol; + vc-MG, 3 d after transfer of 10^5 BV-2 control vector-control microglial cells; + asPARP-1-MG, 3 d after transfer of 10^5 antisense PARP-1 BV-2 microglial cells. (d) Pictures of propidium iodide fluorescence microscopy of the regions of neuronal injury in the cornu ammonis and dentate gyrus in living organotypic brain slice cultures. 7-KC, 3 d after incubation with 10 mg/liter 7-ketocholesterol; + vc-MG, 3 d after transfer of 10^5 BV-2 control vector-control microglial cells; + asPARP-1-MG, 3 d after transfer of 10^5 antisense PARP-1 BV-2 microglial cells.

concentrations of 7-ketocholesterol found in the CSF of MS patients might be mediated by microglial cells.

Activation of Microglial Cells by 7-Ketocholesterol. Our first experiments addressing the direct effects of 7-ketocholesterol on microglial cells revealed strong activation demonstrated by an amoeboid morphology (Fig. 5 a), an increased proliferation rate (Fig. 5 a), an increased expression of migration-regulating integrins such as CD11a and ICAM-1 in the FACS® analysis (Fig. 5 b), and the induction of iNOS (Fig. 5 c). This was the case with the concentrations found in the CSF of MS patients. However, higher concentrations abolished proliferation and exhibited cytotoxicity (Fig. 5, a and b) as previously described (44). Microglial activation was observed in concentrations distinctly below levels measured in the CSF of MS patients, but reflected the levels in our damage studies (Fig. 2, a–d). These concentrations had already contributed to enhanced CD11a and ICAM-1 expression (Fig. 5 b), and iNOS induction (Fig. 5 c). Microglial activation by nontoxic levels of 7-ketocholesterol was accompanied by translocation of NF-κB (p65; Fig. 5 c) and activation of the PARP in the nucleus (Fig. 5 e), a 113-kD nuclear enzyme, which plays an important regulatory role during the activation of inflammatory cells (27, 45) and is a strong coactivator of NF-κB (46, 47). During this transformation of microglial cells from a resting to a state, 7-ketocholesterol enters the nucleus and is then followed by PARP activation (Fig. 5 e). LPS activation enhances the nuclear uptake by about twofold (Fig. 5 d). Because PARP is already highly active in LPS-stimulated microglial cells, this induced only a slight increase in PARP activity (Fig. 5 e). This implies that 7-ketocholesterol does not induce the inflammatory response of activated microglial cells, but is capable of stimulating microglial cells that are primarily inactive.

Because PARP-1 plays a central role during the conversion of microglial cells from the resting to the activated state (27, 45), the question arises whether the activation of PARP is causally linked with the translocation of 7-ketocholesterol into the nucleus. Thus, we incubated isolated nuclei of ramified BV-2 microglial cells with 7-ketocholesterol using those concentrations as detected in the nucleus (Fig. 5 d) and revealed an immediate and distinct increase of nuclear poly(ADP-ribosyl)ation (Fig. 5 f). To test whether PARP-1 is activated directly or indirectly by 7-ketocholesterol, we incubated isolated recombinant PARP-1 with 7-ketocholesterol in the presence and absence of DNA. 7-ketocholesterol was not capable of activating recombinant PARP-1 by itself, but was capable in the presence of DNA (Fig. 5 g). After a short lag phase of ~10 min, the extent of poly(ADP-ribosyl)ation induced by 7-ketocholesterol in the presence of DNA reached the amount induced by single strand break DNA, suggesting that 7-ketocholesterol activates PARP-1 via modification of DNA.

Down-regulation of Microglial PARP-1 Protects from 7-Ketocholesterol–induced Neuronal Damage in Living Brain Tissue. Because PARP-1 has been identified as a direct downstream molecular target of in vivo concentrations of 7-ketocholesterol, we finally addressed the question of whether down-regulation of PARP-1 might reduce the microglia-mediated neuronal damage in inflamed living brain tissue. BV-2 microglial cells stably transfected with an antisense PARP-1-pcDNA3.1 vector (antisense-PARP-1; reference 27) failed to respond with integrin CD11a and ICAM-1 expression after incubation with 7-ketocholesterol (Fig. 6 a). These findings indicate that 7-ketocholesterol acts via a signaling pathway involving PARP-1 activation. As a consequence, although control vector–transfected BV-2 microglial cells migrated specifically inside the neuronal layers of living brain tissue in the presence of 7-ketocholesterol, antisense PARP-1-BV-2 microglial cells were no longer capable of migrating site specifically (27, 29; Fig. 6 b). The invasion of antisense PARP-1-BV-2 microglial cells resulted in only 58% cell death within the neuronal layers of the hippocampus compared with control vector–transfected BV-2 microglial cells (Fig. 5, c and d). This indicates that 7-ketocholesterol–induced PARP-1 activation in migrating microglia cells contributes significantly to the extent of neuronal damage after inflammatory decomposition of cholesterol in myelin sheaths or cell membranes.

Discussion

Our initial finding that the CSF of MS patients contained highly elevated concentrations of the reportedly neurotoxic cholesterol breakdown product 7-ketocholesterol, led us to speculate that this phenomenon plays an important role in perpetuating neuronal damage, which is assumed to be an important feature in the course of MS (1–10). Here, we provide evidence that 7-ketocholesterol released during inflammatory demyelination in the course of MS indirectly induces neuronal damage mediated by activated microglial cells. Transformation of microglial cells from the resting to the activated state by 7-ketocholesterol involved the translocation of NF-κB and the activation of PARP-1, which in turn regulates the expression of the iNOS, CD11a, and ICAM-1, and is crucial for microglial migration. Recently, we showed that latter mechanisms are essential for the damaging activity of microglial cells (27). Importantly, the cascade of 7-ketocholesterol–induced neuronal damage via PARP-1 activation in microglial cells obviously occurs beyond the primary MS inflammation. Myelin damage induced by the initial T cell invasion in MS might result in the release of 7-ketocholesterol found in MS patients, and subsequently trigger a sustained chain of detrimental reactions toward neurons, finally independent of the primary event. Microglial cells are capable of acting as the crucial mediator for this toxic effect because 7-ketocholesterol triggers PARP-1–dependent microglial activation and migration in the absence of a primary inflammatory stimulus. Such a mechanism downstream from the T cell response may play an important role in sustaining neuronal damage in MS. On the other hand, an intervention in these secondary inflammatory and self-sustaining damage

cascades offers an interesting therapeutic option to delay the clinical onset and progress of neurodegeneration, in particular if the primary and initial pathological event is still unknown or difficult to treat. Here we uncovered a possible direct molecular link between demyelination and neuronal damage during MS and identified the microglial PARP-1 as crucial in this damage cascade.

We thank Mrs. Brita Scholte for her excellent technical assistance and Mrs. Rossegger for her skillful secretarial assistance. We thank the University of Miami Human Brain Bank (Dr. C. Petito, N01-H0-8-3284) and the Manhattan Brain Bank (Dr. S. Morgello, R24MH59724) for normal human brain samples.

This study was supported by a grant from the Deutsche Forschungsgemeinschaft to O. Ullrich, F. Zipp, and R. Nitsch (SFB 507/C6, B14 and B11), National Institutes of Health grants NS 08952 and NS 11920 to C.S. Raine, and grants to F. Zipp (Bundesministerium für Bildung und Forschung and Gemeinnützige Hertie-Stiftung).

Submitted: 13 June 2003
Accepted: 22 October 2003

References

1. Trapp, B.D., J. Peterson, R.M. Ransohoff, R.A. Rudick, S. Mork, and L. Bo. 1998. Axonal transection in the lesions of multiple sclerosis. *N. Engl. J. Med.* 338:278–285.
2. Pitt, D., P. Werner, and C.S. Raine. 2000. Glutamate excitotoxicity in a model of multiple sclerosis. *Nat. Med.* 6:67–70.
3. Smith, T., A. Groom, B. Zhu, and L. Turski. 2000. Autoimmune encephalomyelitis ameliorated by AMPA antagonists. *Nat. Med.* 6:62–66.
4. Kornek, B., M.K. Storck, R. Weissert, E. Wallstroe, A. Stefferl, T. Olsson, C. Linington, M. Schmidbauer, and H. Lassmann. 2000. Multiple sclerosis and chronic autoimmune encephalomyelitis: a comparative quantitative study of axonal injury in active, inactive, and remyelinated lesions. *Am. J. Pathol.* 157:267–276.
5. Peterson, J.W., L. Bo, S. Mork, A. Chang, and B.D. Trapp. 2001. Transected neurites, apoptotic neurons, and reduced inflammation in cortical multiple sclerosis lesions. *Ann. Neurol.* 50:389–400.
6. Ferguson, B., M.K. Matyszak, M.M. Esiri, and V.H. Perry. 1997. Axonal damage in acute multiple sclerosis lesions. *Brain.* 120:393–399.
7. Coles, A.J., M.G. Wing, P. Molyneux, A. Paolillo, C.M. Davie, G. Hale, D. Miller, H. Waldmann, and A. Compston. 1999. Monoclonal antibody treatment exposes three mechanisms underlying the clinical course of multiple sclerosis. *Ann. Neurol.* 46:296–304.
8. Bjartmar, C., R.P. Kinkel, G. Kidd, R.A. Rudick, and B.D. Trapp. 2001. Axonal loss in normal-appearing white matter in a patient with acute MS. *Neurology.* 57:1248–1252.
9. Bjartmar, C., and B.D. Trapp. 2001. Axonal and neuronal degeneration in multiple sclerosis: mechanisms and functional consequences. *Curr. Opin. Neurol.* 14:271–278.
10. Bjartmar, C., G. Kidd, S. Mork, R. Rudick, and B.D. Trapp. 2000. Neurological disability correlates with spinal cord axonal loss and reduced N-acetyl aspartate in chronic multiple sclerosis patients. *Ann. Neurol.* 48:893–901.
11. Hemmer, B., J.J. Archelos, and H.-P. Hartung. 2002. New concepts in the immunopathogenesis of multiple sclerosis. *Nat. Rev. Neurosci.* 3:291–301.
12. Smith, K.J., R. Kapoor, and P.A. Felts. 1999. Demyelination: the role of reactive oxygen and nitrogen species. *Brain Pathol.* 9:69–92.
13. Bongarzone, E.R., J.M. Pasquini, and E.F. Soto. 1995. Oxidative damage to proteins and lipids of CNS myelin produced by in vitro generated reactive oxygen species. *J. Neurosci. Res.* 41:213–221.
14. Lizard, G., M. Moisant, C. Cordelet, S. Monier, P. Gambert, and L. Lagrost. 1997. Induction of similar features of apoptosis in human and bovine vascular endothelial cells treated by 7-ketocholesterol. *J. Pathol.* 183:330–338.
15. Lizard, G., V. Deckert, L. Dubrez, M. Moisant, P. Gambert, and L. Lagrost. 1996. Induction of apoptosis in endothelial cells treated with cholesterol oxides. *Am. J. Pathol.* 148:1625–1638.
16. Zhou, Q., E. Wasowicz, B. Handler, L. Fleischer, and F.A. Kummerow. 2000. An excess concentration of oxysterols in the plasma is cytotoxic to cultured endothelial cells. *Atherosclerosis.* 149:191–197.
17. Chang, J.Y., and L.Z. Liu. 1998. Neurotoxicity of cholesterol oxides on cultured cerebellar granule cells. *Neurochem. Int.* 32:317–323.
18. Chang, J.Y., K.D. Phelan, and J.A. Chavis. 1998. Neurotoxicity of 25-OH-cholesterol on sympathetic neurons. *Brain Res. Bull.* 45:615–622.
19. Chang, J.Y., K.D. Phelan, and L.Z. Liu. 1998. Neurotoxicity of 25-OH-cholesterol on NGF-differentiated PC12 cells. *Neurochem. Res.* 23:7–16.
20. Poser, C.M., D.W. Paty, L. Scheinberg, W.I. McDonald, F.A. Davis, G.C. Ebers, K.P. Johnson, W.A. Sibley, D.H. Silberberg, and W.W. Tourtellotte. 1983. New diagnostic criteria for multiple sclerosis: guidelines for research protocols. *Ann. Neurol.* 13:227–231.
21. Raine, C.S. 1997. Demyelinating diseases. *In* Textbook of Neuropathology (Third Edition). R.L. Davis, and D.M. Robertson, editors. Williams and Wilkins, Baltimore. 243–286.
22. Sevanian, A., R. Seraglia, P. Traldi, P. Rossato, F. Ursini, and H. Hodis. 1994. Analysis of plasma cholesterol oxidation products using gas- and high-performance liquid chromatography/mass spectrometry. *Free Radic. Biol. Med.* 17:397–409.
23. Kritharides, L., W. Jessup, J. Gifford, and R.T. Dean. 1993. A method for defining the stages of low-density lipoprotein oxidation by the separation of cholesterol- and cholesteryl ester-oxidation products using HPLC. *Anal. Biochem.* 213:79–89.
24. Raine, C.S. 1984. Biology of disease. The analysis of autoimmune demyelination: its impact upon multiple sclerosis. *Lab. Invest.* 50:608–635.
25. Brocke, S., A. Gaur, C. Piercy, A. Gautam, K. Gijbels, C.G. Fathman, and L. Steinman. 1993. Induction of relapsing paralysis in experimental autoimmune encephalomyelitis by bacterial superantigen. *Nature.* 365:642–644.
26. Bocchini, V., R. Mazzolla, R. Barluzzi, E. Blasi, P. Sick, and H. Kettenmann. 1992. An immortalized cell line expresses properties of activated microglial cells. *J. Neurosci. Res.* 31: 616–621.
27. Ullrich, O., A. Diestel, I.Y. Eyüpoglu, and R. Nitsch. 2001. Regulation of microglial expression of integrins by poly(ADP-ribose)polymerase-1. *Nat. Cell Biol.* 3:1035–1042.
28. Emig, S., D. Schmalz, M. Shakibaei, and K. Buchner. 1995.

The nuclear pore complex protein p62 is one of several sialic acid-containing proteins of the nuclear envelope. *J. Biol. Chem.* 270:13787–13793.
29. Hailer, N.P., J.D. Jarhult, and R. Nitsch. 1996. Resting microglia cells in vitro: analysis of morphology and adhesion molecule expression in organotypic hippocampal slice cultures. *Glia.* 18:319–331.
30. Murakami, H., N. Tamasawa, J. Matsui, M. Yasujima, and T. Suda. 2000. Plasma oxysterols and tocopherol in patients with diabetes mellitus and hyperlipidemia. *Lipids.* 35:333–338.
31. Dzeletovic, S., O. Breuer, E. Lund, and U. Diczfalusy. 1995. Determination of cholesterol oxidation products in human plasma by isotope dilution mass-spectrometry. *Anal. Biochem.* 225:73–80.
32. Dyer, R.G., M.W. Stewart, J. Mitcheson, K. George, M.M. Alberti, and M.F. Laker. 1997. 7-Ketocholesterol, a specific indicator of lipoprotein oxidation, and malonaldehyde in non-insulin dependent diabetes and peripheral vascular disease. *Clin. Chim. Acta.* 260:1–13.
33. Addis, P.B., H.A. Emanuel, S.D. Bergmann, and J.H. Zayoral. 1989. Capillary GC quantification of cholesterol oxidation products in plasma lipoproteins of fasted humans. *Free Radic. Biol. Med.* 7:179–182.
34. Posse de Chaves, E.I., D.E. Vance, R.B. Campenot, R.D. Kiss, and J.E. Vance. 2000. Uptake of lipoproteins for axonal growth of sympathetic neurons. *J. Biol. Chem.* 275:19883–19890.
35. Bondy, S.C., and D.K. Lee. 1993. Oxidative stress induced by glutamate receptor agonists. *Brain Res.* 610:229–233.
36. Maor, I., M. Kaplan, T. Hayek, J. Vaya, A. Hoffman, and M. Aviram. 2000. Oxidized monocyte-derived macrophages in aortic atherosclerotic lesion from apolipoprotein E-deficient mice and from human carotid artery contain lipid peroxides and oxysterols. *Biochem. Biophys. Res. Commun.* 269:775–780.
37. Mattson, M.P., S.W. Barger, J.G. Begley, and R.J. Mark. 1995. Calcium, free radicals, and excitotoxic neuronal death in primary cell culture. *Methods Cell Biol.* 46:187–216.
38. Braun, J.S., R. Novak, K.H. Herzog, S.M. Bodner, J.L. Cleveland, and E.I. Tuomanen. 1999. Neuroprotection by a caspase inhibitor in acute bacterial meningitis. *Nat. Med.* 5:298–302.
39. Miller, S.D., and W.J. Karpus. 1994. The immunopathogenesis and regulation of T cell-mediated demyelinating diseases. *Immunol. Today.* 15:356–361.
40. Zamvil, S.S., and L. Steinman. 1990. The T lymphocyte in experimental allergic encephalomyelitis. *Annu. Rev. Immunol.* 8:579–621.
41. Martin, R., H.F. McFarland, and D.E. McFarlin. 1992. Immunological aspects of demyelinating diseases. *Annu. Rev. Immunol.* 10:153–187.
42. Noseworthy, J.H., C.F. Lucchinetti, M. Rodriguez, and B.G. Weinshenker. 2000. Multiple sclerosis. *N. Engl. J. Med.* 343:938–952.
43. Goverman, J., and T. Brabb. 1996. Rodent models of experimental allergic encephalomyelitis applied to the study of multiple sclerosis. *Lab. Anim. Sci.* 46:482–492.
44. Chang, J.Y., J.A. Chavis, L.Z. Liu, and P.D. Drew. 1998. Cholesterol oxides induce programmed cell death in microglial cells. *Biochem. Biophys. Res. Commun.* 249:817–821.
45. Chiarugi, A., and M.A. Moskowitz. 2003. Poly(ADP-ribose) polymerase-1 activity promotes NF-kappaB-driven transcription and microglial activation: implication for neurodegenerative disorders. *J. Neurochem.* 85:306–317.
46. Hassa, P.O., and M.O. Hottiger. 2002. The functional role of poly(ADP-ribose)polymerase-1 as novel coactivator of NF-kappaB in inflammatory disorders. *Cell. Mol. Life Sci.* 59: 1534–1553.
47. Hassa, P.O., M. Covic, S. Hasan, R. Imhof, and M.O. Hottiger. 2001. The enzymatic and DNA binding activity of PARP-1 are not required for NF-kappaB coactivator function. *J. Biol. Chem.* 276:45588–45597.